Desalination and Water Treatment
www.deswater.com
doi: 10.1080/19443994.2013.833873

52 (2014) 2678–2687
March

Taylor & Francis
Taylor & Francis Group

Adsorption of tetracycline and ciprofloxacin on activated carbon prepared from lignin with H_3PO_4 activation

Lihui Huang*, Man Wang, Cuixia Shi, Ji Huang, Bo Zhang

Shandong Provincial Key Laboratory of Water Pollution Control and Resource Reuse, School of Environmental Science and Engineering, Shandong University, Jinan 250100, China
Tel. +86 531 88366873; Fax: +86 531 88364513; email: huanglihui9986@126.com

Received 28 April 2013; Accepted 16 July 2013

ABSTRACT

Adsorption of tetracycline (TC) and ciprofloxacin (CPX) onto activated carbon prepared from lignin by H_3PO_4 impregnated was investigated. Lignin-activated carbon (LGAC) was carbonized at 450°C in a muffle furnace for 1 h. Scanning electron microscope, N_2 adsorption–desorption isotherms, X-ray diffraction, pH at the point of zero charge and Boehm titration analysis need to characterize the properties of LGAC. Batched adsorption experiments were performed to study the adsorption properties and interaction mechanisms between TC/CPX and LGAC. The prepared activated carbon was found to have a porous structure with surface area of 931.53 m^2/g and many functional groups (acidic groups, basic groups). The adsorption kinetics for the two adsorbates both well fitted the pseudo-second-order model ($R^2 > 0.99$). Compared with Temkin isotherm and Freundlich isotherm, the adsorption equilibrium data were very well represented by the Langmuir isotherm. The maximum adsorption capacities for the TC and CPX calculated by the Langmuir isotherm model were high at 475.48 and 418.60 mg/g, respectively. Thermodynamics study showed that the adsorption was spontaneous and favorable. These results suggested that LGAC could be an effective adsorbent for removal of TC and CPX.

Keywords: Activated carbon; Adsorption kinetics and isotherm; Ciprofloxacin; Desorption; Lignin; Tetracycline

1. Introduction

Antibiotics have been extensively used in human therapy and veterinary treatment [1]. Tetracycline (TC), due to having the stable naphthol ring as its main structure, provides broad-spectrum antimicrobial activity [2]. In China, the annual TC usage was about 9,413 tons in 1999 and the TC production was around 10,000 tons in 2003 [3]. In the mean time, ciprofloxacin (CPX), one of the quinolone antibiotics [4] has been detected with much higher concentrations in effluents from hospitals (3–87 μg/L) than concentrations (<1 μg/L) typically found in water and wastewater [5]. These antibiotics are applied to treat bacterial infections, and their incomplete metabolism in humans and animals discharged into environment [6,7]. The excreted residual amounts released into surface water or groundwater bring about environmental pollution and health problems [8]. Moreover, the toxicity of degradation byproducts of antibiotics is possibly much stronger than their parents [9,10],

*Corresponding author.

which yet in low concentrations, may be lead to the growth of antibiotic-resistant bacteria [11]. Therefore, removal of antibiotics from environment is highly urgent to reduce the potential health, social and ecological risk.

Activated carbon, with a large surface area, well-developed porous structure and ample functional groups, has been widely used in removing organic and inorganic pollutants from aqueous phase [12,13]. Currently, main raw materials for producing activated carbons are high-cost materials, such as wood [14] and coal [15]. Taking advantage of activated carbon for wastewater treatment is often restricted because of the economical consideration. Therefore, manufacturing activated carbon economically is of great interest. Lignin is abundant in black liquors of paper mills whose pulping process produce wastewater [16]. Using lignin as raw material for preparing activated carbon [17] could reduce the disposal and treatment cost of black liquors. Limited researches have been conducted in this area.

The objective of this study was to prepare activated carbon from lignin (LGAC) for two adsorbents (TC and CPX) removal from aqueous solution. Physical and chemical properties of LGAC were investigated by scanning electron microscope (SEM) analysis, N_2 adsorption/desorption isotherms, X-ray diffraction (XRD), point of zero charge (pH_{pzc}), and Boehm titration. The adsorption behavior of two adsorbates (TC and CPX) on the activated carbon was explored, and kinetics and thermodynamics study were used to describe several important thermodynamic parameters. In addition, desorption studies were performed to calculate regeneration capacity.

2. Materials and methods

2.1. Chemicals

All the reagents used were of analytical grade. The two antibiotic adsorbates were TC hydrochloride (98.5% is purity, CAS#: 64-75-5) and CPX hydrochloride (98.5% is purity, CAS#: 3810-74-0) purchased from Sangon Biotech (Shanghai) Co., Ltd. The stock adsorbate solutions were prepared by dissolving accurately weighed amounts of the antibiotics in distilled water.

2.2. Adsorbent preparations

Lignin (purity >95%), purchased from Zibo Splendor Refractory Material Co., Ltd. Shandong in east China, was dried at 105°C for 8 h, then immersed in 40 wt.% H_3PO_4 solution at a ratio of 1:2 (g lignin/g H_3PO_4) for 12 h. The impregnated sample was heated in a muffle furnace to the desired temperature of 450°C for 1 h. After cooling to room temperature, the carbon was washed with distilled water until near neutral pH and dried at 80°C for 12 h. The dried samples were then crushed using a grinder. Particles with sizes of 0.1–0.15 mm (100–140 mesh) referred to as LGAC was used in subsequent experiments.

2.3. Characterization methods

The morphologies of activated carbon were analyzed by SEM (JEOL JSM-7600F). The Brunauer–Emmett–Teller (BET) surface area and porous properties were measured by N_2 adsorption/desorption isotherms at 77 K using a surface area analyzer (Quantachrome Corporation, USA). The surface area was obtained from BET theory, and the pore size distribution of LGAC was derived from Density Functional Theory method. The surface area (S_{BET}) and the total pore volume (V_{tot}) were obtained from the manufacturer's software by the BET theory and BJH theory, respectively. The *t*-plot method was used to calculate the micropore surface area (S_{mic}) and micropore volume (V_{mic}). The mesopore volume (V_{ext}) was obtained by V_{mic} from V_{tot} and the external area (S_{ext}) was the deduction of S_{mic} from S_{BET}. D_P, the mean pore diameter, was calculated from $D_P = 4V_{tot}/S_{BET}$.

XRD was used to identify the crystal phases of the adsorbent. The patterns of which were recorded on the Rigaku D/MAX-YA diffractometer with Ni-filtered Cu Kα radiation as the X-ray source.

The pH_{pzc} was estimated from a batch of equilibrium method described by Babić and Faria [18,19]. The initial pH ($pH_{initial}$) was adjusted with NaOH and HCl to the desired values between 2 and 14. The each conical flask with 20 mg activated carbon was placed in a shaker for 24 h, and pH of the solution was regarded as pH_{finial}. The pH_{pzc} value was a point where $pH_{initial} = pH_{finial}$.

The content of acidic and basic functional groups on the surface of LGAC was determined by Boehm titration method [20]. Boehm titration can be considered as an effective method for evaluating the amount of surface functional groups of LGAC. A series of 0.5 g of LGAC were placed in 25 mL of the following solution [21]: NaOH (0.1 N), Na_2CO_3 (0.1 N), $NaHCO_3$ (0.1 N) and HCl (0.1 N), and then the mixture was placed in a temperature-controlled water bath at 20 ± 1°C for 24 h. After filtration, the excess base or acid was titrated with 0.1 N HCl or NaOH. The quantity of functional groups was determined under the assumptions that $NaHCO_3$ neutralized only carboxylic groups, Na_2CO_3 neutralizes carboxylic and lactonic

groups, NaOH neutralizes carboxylic, lactonic and phenolic groups, and HCl neutralizes basic groups.

2.4. Adsorption experiments

2.4.1. Adsorption equilibrium experiments

Batch equilibrium sorption experiments were carried out in 250 mL Erlenmeyer flasks at a constant temperature (293 K). A dose of LGAC (0.1 g) was put into each Erlenmeyer flask, containing 100 mL of TC (or CPX) solutions of initial concentrations (TC: 180–600 mg/L; CPX: 180–600 mg/L). Then, the solution was shaken in a constant temperature water bath at 150 rpm until the equilibrium was reached. Then, the samples were filtered using 0.45 μm millipore membrane filters and the concentrations of filtrates were analyzed by a UV-visible spectrophotometer (UV-754, Shanghai) at their maximum absorption wavelength of 355 nm for TC and 270 nm for CPX.

2.4.2. Adsorption kinetic experiments

Adsorption kinetic experiments were carried out to investigate the effect of contact time and to evaluate the kinetic properties. LGAC (1.0 g) was added into 1 L of antibiotics solution with initial concentrations (TC: 320 and 420 mg/L; CPX: 320 and 400 mg/L). The mixture was agitated at a speed of 300 rpm on an electromagnetic stirrer (Model 78-1) at 20 ± 1 ℃. At preset time intervals (0–24 h), 10 mL samples were obtained and filtered, and the residual antibiotics concentration was determined. The adsorption capacity q_t (mg/g) was calculated by the equation below:

$$q_t = (C_0 - C_t)V/W \tag{1}$$

where C_0 and C_t (mg/L) are the initial and time t concentrations of TC or CPX, respectively; V (L) represents the volume of the solution; W (g) is the weight of the adsorbent.

2.5. Desorption experiments

After the kinetics study, the spent activated carbon was filtered, washed and dried in a vacuum oven at 80 ℃. As desorption agents, 0.01 N HCl, 0.05 N HCl, 0.01 N NaOH, and 0.05 N NaOH were used. The percentage of desorption was calculated using the following equation:

$$\text{Desorption } (\%) = \frac{C_{de}}{C_{ad}} \times 100\% \tag{2}$$

where C_{de} is the amount of antibiotics desorbed (mg/L); C_{ad} is the amount of antibiotics adsorbed (mg/L).

2.6. Applied models

2.6.1. Kinetics models

In order to elucidate the mechanism, the kinetic data for the adsorption of TC and CPX onto LGAC were analyzed with the pseudo-second-order model, the Elovich equation and intra-particle diffusion model.

The pseudo-second-order model assumes that the adsorption progress is affected by chemical interactions which contribute to binding of the adsorbate onto the adsorbent surface [22]. The integral form of the pseudo-second-order model can be written as [23]:

$$q_t = \frac{k{q_e}^2 t}{1 + kq_e t} \tag{3}$$

where q_e and q_t (mg/g) are the amounts of TC or CPX adsorbed on the adsorbent in equilibrium and at time t, respectively; k (g/(mg min)) is the pseudo-second-order model rate constant. It can be rearranged into a linear form [24]:

$$\frac{t}{q_t} = \frac{1}{k{q_e}^2} + \frac{1}{q_e}t \tag{4}$$

The Elovich equation, which corresponding to the pseudo-second-order model, has been widely used in adsorption kinetics and it describes the mechanism of chemisorptions (chemical reaction) in nature. The Elovich model [25,26] can be written as:

$$q_t = a\ln(t) + b \tag{5}$$

where a (mg/(g min)) and b (g/mg) are empirical constants, the constant a is regarded to relate to the initial rate.

To explain the rate controlling step in multistep adsorption processes, the intra-particle diffusion model was represented as the following equation [27]:

$$q_t = k_{pi}t^{1/2} + C_i \tag{6}$$

where k_{pi} (mg/(g min$^{1/2}$)) is the rate constant of intra-particle diffusion model, and C_i gives an idea about the thickness of boundary layer. A plot of q_t vs. $t^{1/2}$ could determine the values of k_{pi} and C_i.

This model presumes when q_t and $t^{1/2}$ shows a good linear relationship through origin; intra-particle

diffusion model is the sole rate-limiting step and there may be a possibility of transport adsorbate into the pores of adsorbent.

2.6.2. Isotherms models

Adsorption isotherms are helpful to describe how adsorbates interact with adsorbents when the adsorption process reaches equilibrium, and thus are critical for analyzing the equilibrium characteristics at various temperatures. Three widely used models, the Langmuir, Temkin, and Freundlich isotherm model, were applied to analyze the adsorption of antibiotics onto LGAC.

The Langmuir isotherm is based on the monolayer adsorption: the adsorbate distributed homogenously on the surface [28] while no interaction existed between the adsorbate molecules. The general Langmuir isotherm equation is described as follows [29]:

$$q_e = \frac{Q_m K_L C_e}{1 + K_L C_e} \tag{7}$$

$$\frac{C_e}{q_e} = \frac{1}{Q_m K_L} + \frac{1}{Q_m} C_e \tag{8}$$

where q_e (mg/g) is the amount of adsorbate adsorbed under equilibrium; C_e (mg/L) is the equilibrium concentration of TC/CPX; and Q_m (mg/g) represents the theoretical maximum adsorption amount adsorbed corresponding to the complete monolayer coverage; K_L (L/mg) is the Langmuir adsorption constant; Q_m and K_L are determined from the flowing linear form of the equation.

The Temkin isotherm model [30] suggests that the heat of adsorption of all the molecules in the layer would decrease linearly with coverage owing to indirect adsorbent–adsorbate interactions [31] and the binding energies distributed uniformly. The Temkin isotherm in its linear form can be expressed:

$$q_e = B \ln K_T + B \ln C_e \tag{9}$$

where B is the Tempkin constant which related to heat of adsorption; K_T (L/mg) is the equilibrium binding constant; and B and K_T can be determined from the slope and intercept of the plot.

The Freundlich isotherm model is employed to describe heterogeneous adsorbent surface and not restricted to monolayer formations, which is different from the Langmuir isotherm model. The Freundlich equation [32] can be shown as:

$$q_e = K_F C_e^{1/n} \tag{10}$$

where q_e (mg/g) is the adsorption capacity at equilibrium; C_e (mg/L) is the equilibrium concentration of the antibiotics; K_F (mg/g·(L/mg)$^{1/n}$) is the empirical constant of adsorption capacity; n presents the adsorption intensity, giving an indication of how favorable the adsorption process, which assesses the poor adsorption ($n<1$) or preferential adsorption ($n>1$). The linear form of the equation is as follows [4]:

$$\ln q_e = \ln K_F + \frac{1}{n} \ln C_e \tag{11}$$

2.6.3. Adsorption thermodynamics

The thermodynamic parameters, including the free energy changes (ΔG° (kJ/mol)), the standard enthalpy changes (ΔH° (kJ/mol)) and the entropy changes (ΔS° (kJ/mol)), were calculated to evaluate the exothermic nature of the adsorption process. The Gibbs free energy change of the process is related to the Langmuir isotherm equilibrium constant (K) by the following equation [33]:

$$\Delta G = -RT \ln K \tag{12}$$

$$\Delta G = \Delta H - T\Delta S \tag{13}$$

where R is the ideal gas law constant (8.314 J/(mol K)); T (K) is the absolute temperature; and K (L/mol) is Langmuir adsorption constant. The value of ΔG was obtained from above equation, and the values of ΔS and ΔH were determined from the slope and the intercept on the plot of ΔG vs. T.

3. Results and discussion

3.1. Characterization of the LGAC

3.1.1. Surface morphology of LGAC

The SEM micrograph (50,000×magnification) of LGAC is shown in Fig. 1(a). Plenty of irregular pores were widely distributed on the rough surface. These characteristics resulted from the infiltration of phosphate that facilitated the formation of pore structure during carbonized and they are in favor of diffusion of antibiotic molecules into LGAC.

3.1.2. Pore size distribution of LGAC

The pore size distribution and N_2 adsorption/desorption isotherms are shown in Fig. 2. Given the International Union of Pure and Applied Chemistry

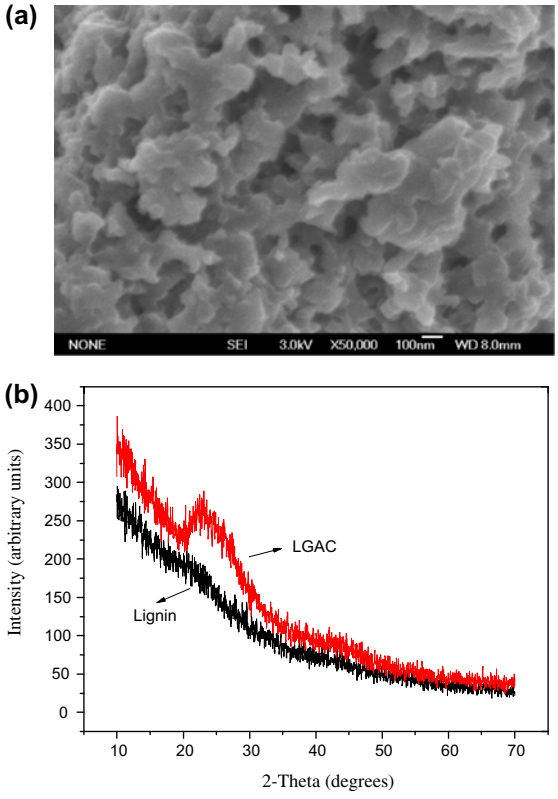

Fig. 1. (a) Scanning electron micrograph of LGAC; (b) XRD profiles of lignin and LGAC.

classification, the adsorbent pores are referred to as three groups: micropore width (<2 nm), mesopore width (2–50 nm), and macropore width (>50 nm) [34]. The N_2 adsorption/desorption isotherms [35] clearly presented the mixture of types I and IV. The initial part of the isotherms followed the same path as the corresponding type I isotherm. The type I isotherm region was quite steep at low P/P_0 and the uptake was limiting owing to microporous substances with narrow pores. Characteristic feature of the type IV is

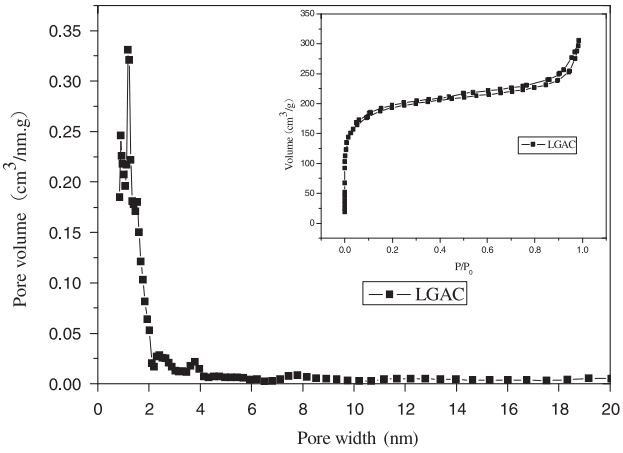

Fig. 2. Pore size distribution of LGAC. The inset is N_2 adsorption/desorption isotherm of LGAC at 77 K.

considered as the monolayer–multilayer adsorption on the mesopore walls. Thus, the adsorption and desorption isotherms revealed the existence of micropores and mesopores simultaneously.

The porous structure parameters for LGAC including the BET surface area and pore volume were calculated in Table 1. The results illustrated that the LGAC was with high surface area of 931.53 m^2/g, and the micropore surface area was 492.91 m^2/g. Both the microspore (62.5%) and mesopore (37.5%) were present in the sample.

3.1.3. XRD analysis of LGAC

The XRD patterns of lignin and LGAC are presented in Fig. 1(b). One strong peak was detected at around 23°, in line with the (002) disordered stacking of micrographites, indicating that the atoms of lignin were in an amorphous phase. The diffraction peak coming in the LGAC might be caused by carbonization and activation process.

Table 1
Textural characterization of LGAC and the Boehm titration and pH_{pzc} results of LGAC

Sample	S_{BET}[a]	S_{ext}[b]		S_{mic}[c]		V_{tot}[d]	V_{ext}[e]		V_{mic}[f]		D_P[i]
	(m^2/g)	(m^2/g)	(%)	(m^2/g)	(%)	(cm^3/g)	(cm^3/g)	(%)	(cm^3/g)	(%)	(nm)
LGAC	931.53	438.62	47.1	492.91	52.9	0.4021	0.1507	37.5	0.2514	62.5	1.18

Sample	pH_{pzc}	Carboxyl (mmol/g)	Lactone (mmol/g)	Phenolic (mmol/g)	Acidic (mmol/g)	Basic (mmol/g)	Total (mmol/g)
LGAC	2.61	2.1966	0	1.7031	3.8977	0.1755	4.0732

[a]BET surface area; [b]external surface area; [c]micropore surface area; [d]total pore volume; [e]mesopore volume; [f]micropore volume; [i]mean pore diameter.

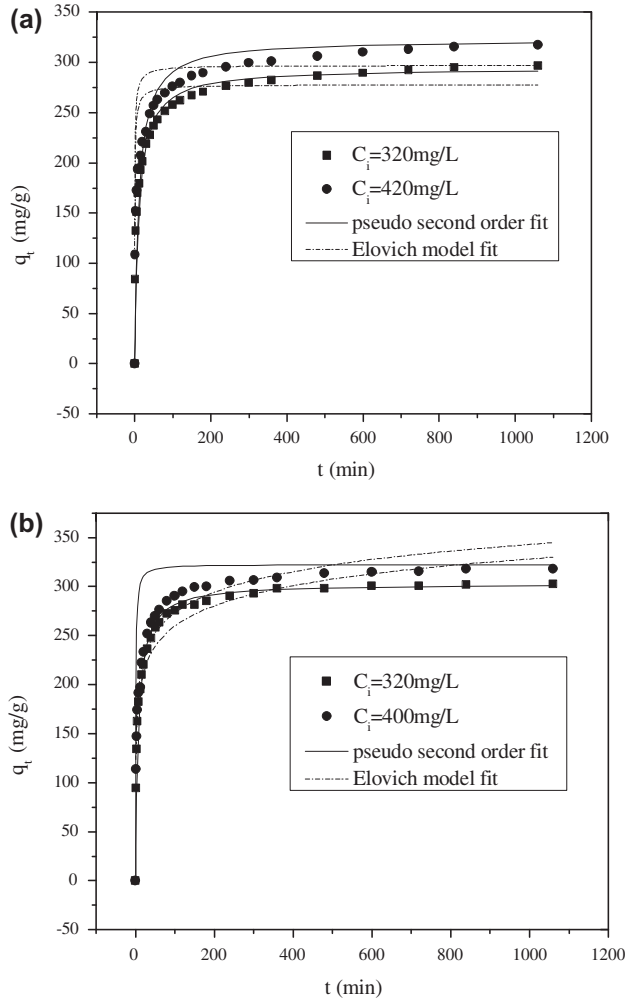

Fig. 3. Effect of contact time and comparison of different kinetic models at different initial concentrations: (a) TC adsorption on LGAC; (b) CPX adsorption on LGAC.

3.1.4. Boehm titration and pH_{pzc} results

As shown in Table 1, there were no lactone groups, and the amount of acidic groups was much larger than the basic ones on the sample surface, and thus the activated carbon was perceived as acidic material. To the best of our knowledge, the acid groups are beneficial for ion exchange and electrostatic adsorption. The pH_{pzc} value was obtained as 2.61, which was consistent to the results of Boehm titration.

3.2. Effect of contact time and adsorption kinetics

Effect of contact time on the adsorption of TC and CPX by LGAC for different initial concentrations was investigated. As shown in Fig. 3, the contact time required to attain equilibrium was about 1,000 min for both TC and CPX. The adsoption rate was quite high initially, and then dropped. Finally, the adsorption capacity for the removal of TC was 317.5 mg/g, compared to CPX 318.1 mg/g.

It can be seen in Fig. 3 that the pseudo-second-order kinetic curves gave a better fit to the experimental kinetic data than the Elovich model. The correlation coefficients and the parameters calculated from the pseudo-second-order model and Elovich model were given in Table 2. The adsorption data agreed well with the two models, indicating that the chemical adsorption occurred in the process.

As Fig. 4 demonstrated, three stages during adsorption process appeared according to the intra-particle diffusion model. The initial curve of the plot indicated that the external mass transferred on the surface of the adsorbent. The second stage implied the intra-particle diffusion was rate-limiting, and the third stage was deemed as the final equilibrium due to little CPX left in solution. Besides, the related parameters including k_{pi}, C_i and R^2 are shown in Table 3. The values of C_i were high; meanwhile, the values of R^2 were greater than 0.9 at different stages, suggesting that the boundary layer might have a great effect on the adsorption behavior. All the results suggested that both surface adsorption and intra-particle diffusion occurred simultaneously during the process.

Table 2
Pseudo-second-order kinetic, Elovich parameter for the adsorption of TC and CPX (LGAC dose = 1 g/L; pH = 5.50 ± 0.03; temperature = 293 K)

Antibiotics	$q_{e,\ exp}$ (mg/g)	Pseudo-second-model parameter			Elovich model parameter		
		$k \times 10^{-3}$ (mg/(g min))	$q_{e,\ cal}$ (mg/g)	R^2	a (mg/(g min))	b (mg/g)	R^2
TC	296.5358	0.3099	294.1176	0.9996	29.94	107.82	0.9659
	317.5121	0.3230	312.5000	0.9995	29.83	127.57	0.9713
CPX	302.5433	0.4356	303.0303	0.9999	29.68	123.19	0.9326
	318.1494	0.4021	322.5806	0.9999	30.15	134.69	0.9360

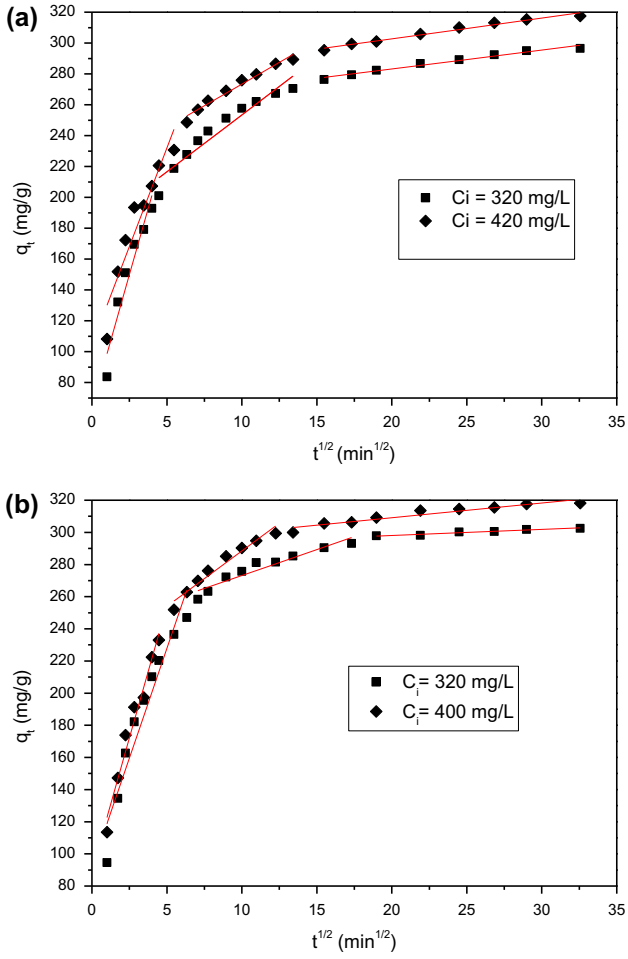

Fig. 4. Intra-particle diffusion equation fit of the adsorption kinetics: (a) TC adsorption; (b) CPX adsorption (LGAC dose = 1g/L; pH = 5.50 ± 0.03; temperature = 293 K).

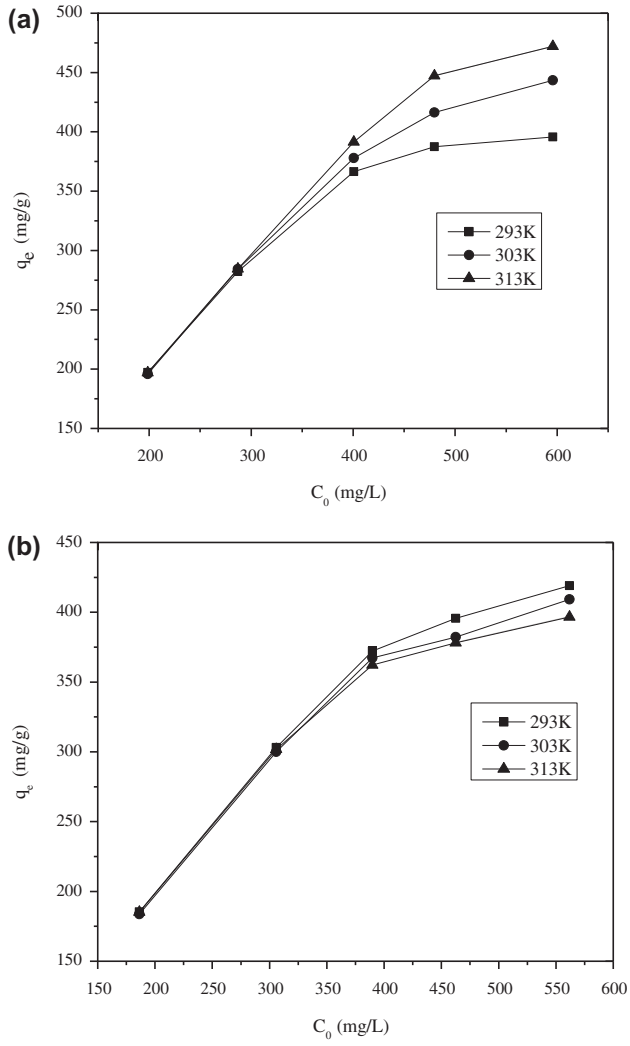

Fig. 5. Effect of temperature and comparison of different isotherm models at three different temperatures: (a) TC adsorption; (b) CPX adsorption (LGAC dose = 1g/L; pH = 5.50 ± 0.03).

3.3. Effect of temperature and adsorption isotherms

In this study, the effect of temperature on adsorption process was investigated at 293, 303, and 313 K. As can be seen from Fig. 5, for TC, the extent of adsorption increased as temperatures rised and the maximal adsorption capacity was up to 473.1 mg/g at 313 K. It seemed that the increase in temperature provided the potential activation energy required to facilitate the TC into the activated complex, thus

Table 3
Intra-particle diffusion model parameters for the adsorption of TC and CPX onto LGAC (LGAC dose = 1 g/L; pH = 5.50 ± 0.03; temperature = 293 K)

Adsorbates	Initial concentrations (mg/L)	The first stage			The second stage			The third stage		
		K_{p1}	C_1	$(R_1)^2$	K_{p2}	C_2	$(R_2)^2$	K_{p3}	C_3	$(R_3)^2$
TC	320	34.153	64.589	0.9288	7.3645	179.78	0.9292	1.2227	258.75	0.9751
	420	25.465	104.650	0.904	5.6205	217.21	0.9715	1.3434	275.85	0.9779
CPX	320	27.289	91.392	0.9276	3.197	237.58	0.9129	0.3718	290.68	0.9473
	400	32.976	89.666	0.9694	6.8718	219.72	0.9578	0.9197	290.7	0.9164

Table 4
Fitted Langmuir, Temkin, Freundlich parameters and correlation for adsorption isotherms (LGAC dose = 1 g/L; pH = 5.50 ± 0.03)

Isotherm models	Constants	TC			CPX		
		293 K	303 K	313 K	293 K	303 K	313 K
Langmuir	Q_m (mg/g)	397.21	444.87	475.48	418.60	407.96	396.32
	K_L (L/mg)	0.7783	0.5749	0.9941	0.8301	0.6877	0.7417
	R^2	0.9998	0.9992	0.9999	0.9993	0.9988	0.9994
Temkin	K_T (L/mg)	6638.99	1061.45	301.48	5625.93	8983.53	3462.87
	B	29.084	37.720	47.883	31.593	29.414	30.857
	R^2	0.9856	0.9782	0.9086	0.9462	0.9531	0.9140
Freundlich	K_F (mg/g (L/mg)$^{1/n}$)	247.9929	253.8897	263.6968	260.2909	255.6732	242.2088
	n	9.9701	8.2102	6.8871	9.2507	9.6993	9.1912
	R^2	0.9648	0.9376	0.8382	0.8924	0.9060	0.8578

Table 5
Comparison of maximum adsorption for TC and CIP on various adsorbents reported in literature

Adsorbent	q_{max} (mg/g)	References
Marine sediments	TC-50.0	[2]
Palygorskite	TC-93.33	[36]
Garphene oxide	TC-313	[37]
LGAC	TC-475.48	This study
Modified coal fly ash	CIP-1.58	[4]
Surface-modified carbon	CIP-300	[5]
2:1 dioctahedral clay minerals	CIP-394.31	[23]
Cyperus alternifolius activated carbon	CIP-377.359	[38]
Arundo donax Linn. activated carbon	CIP-418.41	[39]
LGAC	CIP-418.60	This study

Table 6
Thermodynamic parameters for the uptake of antibiotics on LGAC calculated under standard conditions (LGAC dose = 1 g/L; pH = 5.50 ± 0.03)

Adsorbates	T (K)	ΔG° (kJ/mol)	ΔH° (kJ/mol)	ΔS° (kJ/mol)
TC	293	−31.06837	9.6903	0.1379
	303	−31.36564		
	313	−33.82593		
CPX	293	−30.51003	−4.1836	0.0895
	303	−31.07724		
	313	−32.2996		

enhancing the adsorption capacity by the activated carbon. While for CPX, the adsorption capacity dropped slightly with an increase in temperature, and the maximum uptake was 419.1 mg/g. The values of the constants for the three isotherms are listed in Table 4. The adsorption behavior for TC and CPX fitted the three

models with high correlation coefficients. The equilibrium data were better fitted by the Langmuir equation, when compared to the Temkin and Freundlich equations, suggesting that the adsorption process on LGAC was the single molecule layer adsorption. As shown in Table 4, the n values of the Freundlich isotherm were higher than 1.0 for all temperatures, reflecting that it is favorable for the TC and CPX adsorption onto LGAC. For comparison, Table 5 reveals the maximum adsorption capacity of other adsorbents. A comparison with these adsorbents also demonstrated high TC and CPX adsorption capacity of LGAC and confirmed the suitability for the two antibiotics.

3.4. Adsorption thermodynamics

Thermodynamics parameters are shown in Table 6. The negative values of ΔG° indicated that the adsorption was spontaneous. The absolute values of ΔG° increased with temperature, implying that higher temperature made for the adsorption of the antibiotics on LGAC. The values of ΔS° calculated from the equation were given as 0.1379 and 0.0895 kJ/mol. The positive values of ΔS° informed that the adsorption was spontaneous and favorable. The value of ΔH° (9.6903 kJ/mol) was positive for TC, suggesting that the reaction was endothermic. On the contrary, the negative values of ΔH° (−4.1836 kJ/mol) for CPX indicated an exothermic reaction.

3.5. Desorption studies

Desorption studies are considered as one of the effective methods to evaluate the feasibility of regenerating the spent activated carbon. The desorption rates of 0.01 M HCl, 0.05 M HCl, 0.01 M NaOH, and 0.05 M NaOH were found to be 0.18, 0.29, 22.1 and 22.7% for TC and 3.86, 4.40, 50.57 and 54.52% for CPX. The results indicated that NaOH had better desorption ability, comparing to HCl, implying that the mechanism of TC and CPX adsorption onto LGAC included predominantly chemisorptions with strong bonds.

4. Conclusions

In this study, activated carbon was made from lignin using H_3PO_4 activation and the muffle furnace heating method. LGAC had a large surface area of 931.5 m^2/g, and the amount of acidic surface functional groups (3.8977 mM/g) was much larger than basic groups (0.1755 mM/g). LGAC was an efficient adsorbent for removal of TC and CPX, and the maximum adsorption capacity for TC and CPX, calculated from the Langmuir isotherm model, achieved 475.48 and 418.60 mg/g. Furthermore, the adsorption kinetics for both TC and CPX followed the pseudo-second-order model ($R^2 > 0.99$), implying the sorption rate was controlled by chemical interaction. The adsorption isotherm models fitted the data in the following order: Langmuir > Temkin > Freundlich isotherms. Thermodynamics analyses indicated that the adsorption was spontaneous and favorable, with endothermic nature ($\Delta H^\circ > 0$) of adsorption of TC onto LGAC and exothermic nature ($\Delta H^\circ < 0$) of CPX onto LGAC. The adsorbent is in a good way of renewable and a promising high-efficiency adsorbent for TC and CIP removal.

Acknowledgment

The authors would like to acknowledge financial support for this work provided by Shandong Province Postdoctoral fund.

References

[1] D. Zhang, H.Y. Niu, X.L. Zhang, Z.F. Meng, Y.Q. Cai, Strong adsorption of chlorotetracycline on magnetite nanoparticles, J. Hazard. Mater. 192 (2011) 1088–1093.
[2] X.R. Xu, X.Y. Li, Sorption and desorption of antibiotic tetracycline on marine sediments, Chemosphere 78 (2010) 430–436.
[3] N. Wu, M. Qiao, B. Zhang, W.D. Cheng, Y.G. Zhu, Abundance and diversity of tetracycline resistance genes in soils adjacent to representative swine feedlots in China, Environ. Sci. Technol. 44 (2010) 6933–6939.
[4] C.L. Zhang, G.L. Qiao, F. Zhao, Y. Wang, Thermodynamic and kinetic parameters of ciprofloxacin adsorption onto modified coal fly ash from aqueous solution, J. Mol. Liq. 163 (2011) 53–56.
[5] S.A.C. Carabineiro, T. Thavorn-Amornsri, M.F.R. Pereira, J.L. Figueiredo, Adsorption of ciprofloxacin on surface-modified carbon materials, Water Res. 45 (2011) 4583–4591.
[6] H. Liu, W.F. Liu, J. Zhang, C.L. Zhang, L. Ren, Y. Li, Removal of cephalexin from aqueous solution by original and Cu(II)/Fe(III) impregnated activated carbons developed from lotus stalks kinetics and equilibrium studies, J. Hazard. Mater. 185 (2011) 1528–1535.
[7] V.T. Diwan, A.J. Amhankar, M. Aggarwal, S. Sen, R.K. Khandal, C.S. Lundborg, Detection of antibiotic in hospital effluents in India, Curr. Sci. 97 (2009) 1752–1755.
[8] H.M. Ötker, I. Akmehmet-Balcıoğlu, Adsorption and degradation of enrofloxacin, a veterinary antibiotic on natural zeolite, J. Hazard. Mater. 122 (2005) 251–258.
[9] S.J. Jiao, S.R. Zheng, D.Q. Yin, L.H. Wang, L.Y. Chen, Aqueous photolysis of tetracycline and toxicity of photolytic products to luminescent bacteria, Chemosphere 73 (2008) 377–382.
[10] Y.Y. Sun, Q.Y. Yue, B.Y. Gao, Q. Li, L.H. Huang, F.J. Yao, X. Xu, Preparation of activated carbon derived from cotton linter fibers by fused NaOH activation and its application for oxytetracycline (OTC) adsorption, J. Colloid Interface Sci. 368 (2012) 521–527.
[11] E.M. Golet, A.C. Alder, W. Giger, Environmental exposure and risk assessment of fluoroquinolone antibacterial agents in wastewater and river water of the Glatt Valley Watershed, Switzerland, Environ. Sci. Technol. 36 (2002) 3645–3651.

[12] Y.P. Guo, D.A. Rockstraw, Physical and chemical properties of carbons synthesized from xylan, cellulose, and Kraft lignin by H_3PO_4 activation, Carbon 44 (2006) 1464–1475.
[13] A.A. Ahmad, A. Idris, B.H. Hameed, Organic dye adsorption on activated carbon derived from solid waste, Desalin. Water Treat. 51 (2013) 13–15.
[14] F.C. Wu, R.L. Tseng, R.S. Juang, Preparation of highly microporous carbons from fir wood by KOH activation for adsorption of dyes and phenols from water, Sep. Purif. Technol. 47 (2005) 10–19.
[15] F.C. Wu, P.H. Wu, R.L. Tseng, R.S. Juang, Preparation of activated carbons from unburnt coal in bottom ash with KOH activation for liquid-phase adsorption, J. Environ. Manage. 91 (2010) 1097–1102.
[16] P.J.M. Suhas Carrott, M.M.L. Ribeiro Carrott, Lignin—from natural adsorbent to activated carbon: A review, Bioresour. Technol. 98 (2007) 2301–2312.
[17] L.G. da Silva, R. Ruggiero, P.M. Gontijo, R.B. Pinto, B. Royer, E.C. Lima, T.H.M. Fernandes, T. Calvete, Adsorption of Brilliant Red 2BE dye from water solutions by a chemically modified sugarcane bagasse lignin, Chem. Eng. J. 168 (2011) 620–628.
[18] B.M. Babić, S.K. Milonjić, M.J. Polovina, B.V. Kaludierović, Point of zero charge and intrinsic equilibrium constants of activated carbon cloth, Carbon 37 (1999) 477–481.
[19] P.C.C. Faria, J.J.M. Órfão, M.F.R. Pereira, Adsorption of anionic and cationic dyes on activated carbons with different surface chemistries, Water Res. 38 (2004) 2043–2052.
[20] N.Q. Zhao, N. Wei, J.J. Li, Z.J. Qiao, J. Cui, F. He, Surface properties of chemically modified activated carbons for adsorption rate of Cr(VI), Chem. Eng. J. 115 (2005) 133–138.
[21] O. Hamdaoui, E. Naffrechoux, Modeling of adsorption isotherms of phenol and chlorophenols onto granular activated carbon: Part II. Models with more than two parameters, J. Hazard. Mater. 147 (2007) 401–411.
[22] Y.S. Ho, A.E. Ofomaja, Pseudo-second-order model for lead ion sorption from aqueous solutions onto palm kernel fiber, J. Hazard. Mater. 129 (2006) 137–142.
[23] C.J. Wang, Z.H. Li, W.T. Jiang, Adsorption of ciprofloxacin on 2:1 dioctahedral clay minerals, Appl. Clay Sci. 53 (2011) 723–728.
[24] A.V. Maldhure, J.D. Ekhe, Preparation and characterizations of microwave assisted activated carbons from industrial waste lignin for Cu(II) sorption, Chem. Eng. J. 168 (2011) 1103–1111.
[25] G.L. Dotto, L.A.A. Pinto, Adsorption of food dyes onto chitosan: Optimization process and kinetic, Carbohydr. Polym. 84 (2011) 231–238.
[26] F.C. Wu, R.L. Tseng, R.S. Juang, Characteristics of Elovich equation used for the analysis of adsorption kinetics in dye-chitosan systems, Chem. Eng. J. 150 (2009) 366–373.
[27] H. Demir, A. Top, D. Bolkose, S. Ulku, Dye adsorption behavior of *Luffa cylindrica* fibers, J. Hazard. Mater. 153 (2008) 389–394.
[28] Q. Li, Q.Y. Yue, Y. Su, B.Y. Gao, H.J. Sun, Equilibrium, thermodynamics and process design to minimize adsorbent amount for the adsorption of acid dyes onto cationic polymer-loaded bentonite, Chem. Eng. J. 158 (2010) 489–497.
[29] W.F. Liu, J. Zhang, C.L. Zhang, L. Ren, Sorption of norfloxacin by lotus stalk-based activated carbon and iron-doped activated alumina: Mechanisms, isotherms and kinetics, Chem. Eng. J. 171 (2011) 431–438.
[30] T.L. Kurth, J.A. Byars, S.C. Cermak, B.K. Sharma, G. Biresaw, Non-linear adsorption modeling of fatty esters and oleic estolide esters via boundary lubrication coefficient of friction measurements, Wear 262 (2007) 536–544.
[31] R.D. Johnson, F.H. Arnold, The Temkin isotherm describes heterogeneous protein adsorption, Biochim. Biophys. Acta, Protein Struct. Mol. Enzymol. 1247 (1995) 293–297.
[32] C.A. Coles, R.N. Yong, Use of equilibrium and initial metal concentrations in determining Freundlich isotherms for soils and sediments, Eng. Geol. 85 (2006) 19–25.
[33] V.K. Gupta, A. Mittal, L. Krishnan, V. Gajbe, Adsorption kinetics and column operations for the removal and recovery of malachite green from wastewater using bottom ash, Sep. Purif. Technol. 40 (2004) 87–96.
[34] K.S.W. Sing, D.H. Everett, R.A.W. Haul, L. Moscou, R.A. Pierotti, J. Rouqerol, T. Siemieniewska, Reporting physisorption data for gas/solid systems with special area and porosity, Pure Appl. Chem. 57 (1985) 603–609.
[35] Z.Y. Ryu, J.T. Zheng, M.Z. Wang, B.J. Zhang, Characterization of pore size distributions on carbonaceous adsorbents by DFT, Carbon 37 (1999) 1257–1264.
[36] P.H. Chang, Z.H. Li, T.L. Yu, S. Munkhbayer, T.H. Kuo, Y.C. Hung, J.S. Jean, K.H. Lin, Sorptive removal of tetracycline from water by palygorskite, J. Hazard. Mater. 165 (2009) 148–155.
[37] Y. Gao, Y. Li, L. Zhang, H. Huang, J. Hu, S.M. Shah, X. Su, Adsorption and removal of tetracycline antibiotics from aqueous solution by graphene oxide, J. Colloid Interface Sci. 368 (2011) 540–546.
[38] Y. Sun, Q. Yue, B. Gao, L. Huang, X. Xu, Q. Li, Comparative study on characterization and adsorption properties of activated carbons with H_3PO_4 and $H_4P_2O_7$ activation employing *Cyperus alternifolius* as precursor, Chem. Eng. J. 181–182 (2012) 790–797.
[39] Y. Sun, Q. Yue, B. Gao, B. Wang, Q. Li, L. Huang, X. Xu, Comparison of activated carbons from *Arundo donax* Linn. with $H_4P_2O_7$ activation by conventional and microwave heating methods, Chem. Eng. J. 192 (2012) 308–314.